arXiv:1207.0986v1 [nucl-th] 4 Jul 2012

Reexamining the "finite-size" effects in isobaric yield ratios using a statistical abrasion-ablation model

C. W. Ma* and H. L. Wei
Department of Physics, Henan Normal University, Xinxiang, 453007 China

Y. G. Ma†
Shanghai Institute of Applied Physics, Chinese Academy of Sciences, Shanghai, 201800 China

(Dated: July 5, 2012)

The "finite-size" effects in isobaric yield ratio (IYR), which is shown in the standard grand-canonical and canonical statistical ensembles (SGC/CSE) method, is found to prevent obtaining the actual values of physical parameters. Due to there is no inputs of neutron and proton density distribution in SGC/CSE, the conclusion of SGC/CSE is doubtable. To investigate wether IYR has the "finite-size" effects, IYR of mirror nuclei are reexamined using a modified statistical abrasion-ablation model. IYR of mirror nuclei in the 140A MeV $^{38\sim52}$Ca + ^{12}C, and ^{72}Zn/^{96}Zr/^{120}Sn + ^{12}C reactions are calculated using a modified statistical abrasion-ablation model. IYR of mirror nucleus in reactions of $^{38\sim52}$Ca increases when the projectile becomes more neutron-rich, but saturates in the reactions of very neutron-rich nucleus. IYR of mirror nuclei in reactions of ^{72}Zn/^{96}Zr/^{120}Sn that have same n/p ratio show no "finite-size" effects. IYR of mirror nuclei is found to depends on the isospin of the projectile rather than the size of reaction system.

PACS numbers: 25.70.Pq, 21.65.Cd, 25.70.Mn, 24.60.-k

I. INTRODUCTION

The yield of fragment is often constructed to extract information of nuclear matter and temperature in heavy-ion collisions (HIC). The double yield ratio of light fragments are constructed as thermometer [1–4]. The scaling of the ratios between isotopic yield in similar reactions, i.e., the isoscaling, is used to study the symmetry energy of hot emitting source in framework of various theoretical models [5–17].

Using a modified Fisher model (MFM) that based on free energy [18, 19], the isobaric yield ratio (IYR) is used to extract the symmetry energy of fragment in HIC near the Fermi energy [20]. The correlations between IYR and energy terms which contribute to the free energy of fragment are constructed to extract physical parameters associated with mass of nucleus [21]. In IYR methods, the energy terms that only depend on mass cancel out, which make it convenient to investigate the symmetry-energy term in mass formula.

Recently, it is discussed that the IYR method, which utilizes only one reaction system, does not provide cancelation or minimization of the effects associated with mass and charge constraints due to the "finite-size" effects in the standard grand-canonical and canonical statistical ensembles (SGC/CSE) [22].

The linear behavior of IYR for the mirror nuclei, which is discussed in Ref. [20–22], is written as,

$$\begin{aligned} IYR(m) = \ln[R(1,-1,A)] &\equiv Y(A,1)/Y(A,-1) \\ &= [\mu_n - \mu_p + 2a_c(Z-1)/A^{1/3}]/T, \end{aligned} \quad (1)$$

where a_c is the Coulomb-energy coefficient, μ_n and μ_p are the chemical potential of neutron and proton, respectively.

The "finite-size" effects of IYR(m) in SGC/CSE, which depend on the volume of reaction system, is discussed to prevent one from obtaining precise information on the nuclear properties using the isobaric ratios method. It's also pointed out that the "finite size" effects are negligible only for system sizes much larger than those actually formed in the experiments [22]. Actually, though the finite effects are believed to be minimized from the n/p ratio fixed source in isoscaling, the finite size effects are still obvious in isoscaling in some models [13].

It's well known the yield of fragment has strong dependence on the isospin of the projectile, and the neutron and proton density distributions inside the projectile. Actually, the neutron and proton density distributions are important inputs in nuclear reaction models, while there is no such information in SGC/CSE [22, 23]. The temperature has a wide distribution due to the strength of collisions, while it is set to a certain value in SGC/CSE. The yields of fragments in SGC/CSE are not shown in Ref. [22]. Considering the density distributions of nuclei involved, SGC/CSE is not a good model to evaluate the yield of fragment, especially in reactions of neutron-rich nucleus. Thus the deduction based on yields of fragments in SGC/CSE may be doubtable. The statistical abrasion-ablation (SAA) model can well reproduce the yield of fragments in HIC induced by neutron-rich nucleus at intermediate energy and relativistic energy [7, 24–26], and it is used to study the isospin effect in HIC. Considering the dependence of yields and the resultant IYR(m) on the isospin of projectile, the "finite-size" effects in IYR(m) shown in SGC/CSE (which depend on the volume of reaction system), can also be explained by the

---

* machunwang@126.com
† ygma@sinap.ac.cn

isospin effect in isotopic yield.

In this article, using the SAA model, the 140A MeV $^{38\sim52}$Ca which have different isospins, and ^{72}Zn/^{96}Zr/^{120}Sn that has same n/p ratio as ^{48}Ca (which have been calculated in Ref. [22]) are calculated to show that IYR(m) depend more on the isospin but not the size of the projectile, *i.e.*, the "finite-size" effects of IYR(m) in SGC/CSE should be explained as the isospin effect.

II. MODEL DESCRIPTION

The SAA model was developed by Brohm and Schmidt to predict isotopic yield in the relativistic energy HIC [24, 27] and modified to describe the intermediate energy HIC [7, 25, 26, 28–30]. It can well reproduce the yields of both the small and large mass fragments in the 140A MeV ^{40,48}Ca+^{9}Be and ^{58,64}Ni+^{9}Be projectile fragmentation [25, 31]. For simplification, only some important formula are listed here since the model is well described in Refs. [24, 26, 27, 30, 32].

The SAA model takes independent nucleus nucleus collisions for participants in an overlap zone of the two colliding nuclei and determines the distributions of abraded neutrons and protons. The colliding nuclei are described to be composed of parallel tubes orienting along the beam direction. Neglecting the transverse motion, the collision is described by independent interactions of tube pairs. Assuming a binomial distribution for the absorbed projectile neutrons and protons in the interaction of a specific pair of tubes, the distributions of the total abraded neutrons and protons can be determined. For an infinitesimal tube in the projectile, the transmission probabilities for neutrons (protons) at a given impact parameter $\vec{b}$ are calculated by

$$t_k(\vec{s}-\vec{b}) = \exp\{-[D_n^T(\vec{s}-\vec{b})\sigma_{nk} + D_n^P(\vec{s}-\vec{b})\sigma_{pk}]\} \quad (2)$$

where D^T is the nuclear-density distribution of the target integrated along the beam direction and normalized by $\int d^2sD_n^T = N^T$ and $\int d^2sD_p^T = Z^T$. With N^T and Z^T refer to the neutron and proton number in the target respectively, the vectors $\vec{s}$ and $\vec{b}$ are defined in the plane perpendicular to beam, and $\sigma_{k'k}$ is the free nucleon-nucleon reaction cross section. The average absorbed mass in the limit to infinitesimal tubes at a given $\vec{b}$ is

$$\begin{aligned} < \Delta A(b) >= &\int d^2sD_n^T(\vec{s})[1-t_n(\vec{s}-\vec{b})] \\ &+ \int d^2sD_p^P(\vec{s})[1-t_p(\vec{s}-\vec{b})] \end{aligned} \quad (3)$$

The proton and neutron density distributions are assumed to be the Fermi-type,

$$\rho_i(r) = \frac{\rho_i^0}{1+\exp(\frac{r-C_i}{t_i/4.4})}, i = n, p \quad (4)$$

where ρ_i^0 is the normalization constant, t_i is the diffuseness parameter, and C_i is half the density radius of the neutron or proton density distribution. The parameters in Eq. (4) can be different for proton and neutron in asymmetric nucleus.

The cross section for a specific isotope can be calculated from

$$\sigma(\Delta N, \Delta Z) = \int d^2bP(\Delta N, b)P(\Delta Z, b), \quad (5)$$

where $P(\Delta N, b)$ and $P(\Delta Z, b)$ are the probability distributions for the abraded neutrons and protons at a given impact parameter b, respectively.

The second stage of the reaction is characterized by the evaporation of particles, of which in the SAA model is described by the conventional statistical model under the assumption of thermal equilibrium in the excited prefragment. The excitation energy of projectile spectator is estimated by a simple relation of $E^* = 13.3 < \Delta A(b) >$MeV, where 13.3 is the mean excitation energy due to an abraded nucleon from the initial projectile [27]. After de-excitation, isotopic yield comparable to experimental result is obtained.

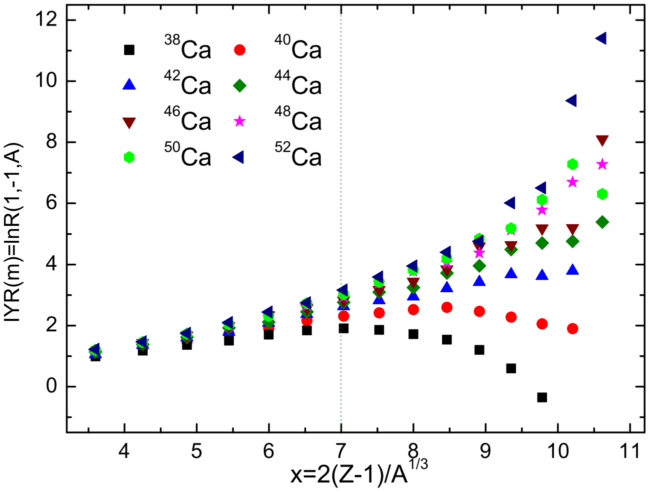

FIG. 1. (Color online) The isobaric yield ratio for mirror nuclei IYR(m) in the 140A MeV $^{38\sim52}$Ca + ^{12}C reactions calculated by the SAA model.

III. RESULTS AND DISCUSSIONS

The isotopic yields in the 140A MeV $^{38\sim52}$Ca + ^{12}C, and ^{72}Zn/^{96}Zr/^{120}Sn+^{12}C reactions are calculated using the SAA model. IYR(m) of the calculated 140 A MeV $^{38\sim52}$Ca + ^{12}C reactions are plotted in Fig. 1. It is found that IYR(m) in the $^{38\sim52}$Ca reactions increase when the projectile nucleus becomes more neutron-rich. Defining $x \equiv 2(Z-1)/A^{1/3}$, when $x < 6$, the difference among IYR(m) of these reactions are quite small. Fairly well linear correlations between IYR(m) and x are found in the ^{42,44}Ca reactions. For the neutron-deficient ^{38}Ca and neutron-proton symmetric ^{40}Ca projectiles, IYR(m) firstly increase linearly with x when $x < 7$, but decrease when $x > 7$. For the neutron-rich $^{46\sim52}$Ca projectiles, IYR(m) increase linearly when x are not large, but IYR(m) increase faster when x of fragments are lager than $0.85x$ of projectile. For these fragments, only few nucleons are removed from the projectile, which are very typical projectile-like fragments. It has been illustrated that these fragments are mostly produced in the peripheral collisions with large impact parameters in the SAA model [33]. The mirror nuclei with small x and large mass x have different production mechanisms. Considering the slopes of the linear correlations [for the linearly increasing part in IYR(m)], the slope increases as neutrons of the projectile increases. For ^{50}Ca and ^{52}Ca, IYR(m) almost overlap except few fragments with large x, which shows the saturation of IYR(m) in reactions induced by the very neutron-rich nuclei.

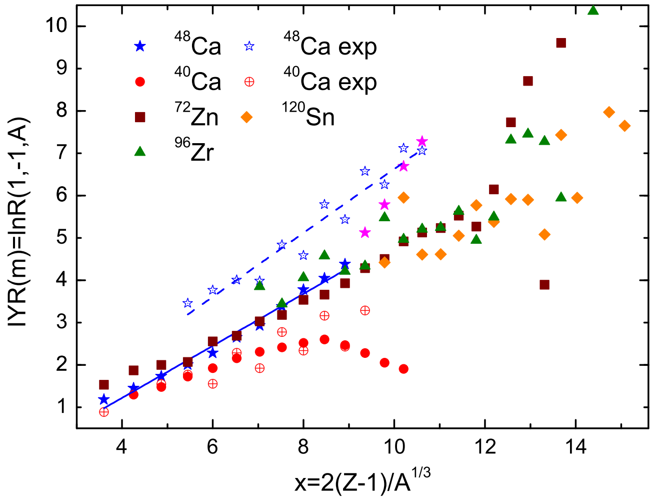

FIG. 2. (Color online) The isobaric yield ratio for mirror nuclei. The full and open circles (stars) are for the SAA and experimental 140A MeV ^{40}Ca(^{48}Ca) induced reactions, respectively; the triangles, hexagon, and diamonds represent IYR(m) for the 140A MeV ^{72}Zn/^{96}Zr/^{120}Sn + ^{12}C reactions. The lines are the linear fitting results by Eq. (1).

In Fig. 2, the SAA calculated and experimental [35] IYR(m) in the 140 A MeV ^{40,48}Ca induced reactions are plotted as the solid and open symbols, respectively. IYR(m) in the 140 A MeV ^{72}Zn/^{96}Zr/^{120}Sn + ^{12}C reactions are also plotted. Though the experimental odd-even staggering in IYR(m) can not be reproduced, the SAA results fit the ^{40}Ca experimental data rather well, including the decreases of IYR(m) when $x > 9$. For ^{48}Ca, the SAA IYR(m) are smaller than the experimental ones. The linear fitting of the SAA and experimental IYR(m) read $y = (0.62 \pm 0.02)x - (1.24 \pm 0.16)$ and $y = (0.75 \pm 0.06)x - (0.92 \pm 0.50)$, respectively. The large difference among IYR(m) in reactions induced by projectiles with same n/p ratio in SGC/CSE disappears in the SAA results. IYR(m) for ^{72}Zn projectile exhibits quite good linear correlation when $x < 11$, which shows very little difference to the IYR(m) for ^{48}Ca. The small mass mirror nuclei do not survive the deexcitation process in SAA calculation for ^{96}Zr and ^{120}Sn, but IYR(m) for ^{72}Zn, ^{96}Zr, and ^{120}Sn show very little difference when $x < 12$. Considering the saturation of IYR(m) in large isospin nucleus induced reactions, the overlap of IYR(m) of ^{72}Zn, ^{96}Zr, and ^{120}Sn can be explained.

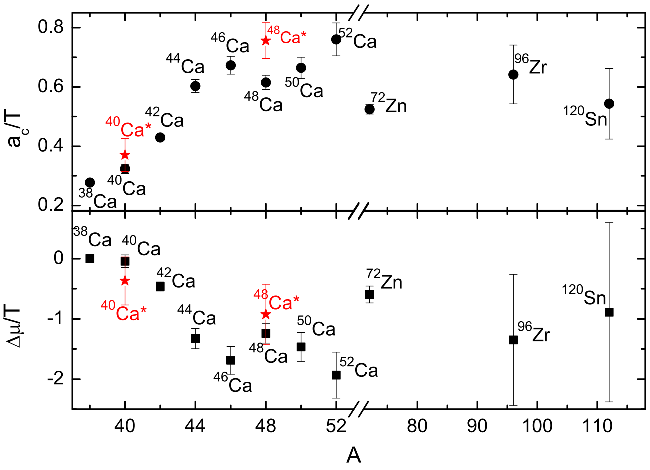

FIG. 3. (Color online) a_c/T and μ/T fitted from IYR(m) by Eq. (1). The labels ^{40}Ca*, ^{48}Ca*, and stars represent the values for the experimental results.

In Fig. 3, the fitted a_c/T and $\Delta\mu$ from IYR(m) in the $^{38\sim52}$Ca and ^{72}Zn/^{96}Zr/^{112}Sn reactions are plotted. The fittings are limited to the linear increasing part of IYR(m). a_c/T ($\Delta\mu/T$) of IYR(m) increases (decreases) when the projectile becomes more neutron-rich, but a_c/T ($\Delta\mu/T$) are similar due to the similar IYR(m) in reactions of the neutron-rich projectiles. For projectile with the same n/p, a_c/T ($\Delta\mu/T$) has very little difference and no finite size effects are shown. It's easy to conclude that IYR(m) depends more on the isospin of the projectile rather than the size of system, and the isospin dependence of a_c/T ($\Delta\mu/T$) is weakened and even disappears in reactions of neutron-rich nucleus.

According to Eq. (5), the yield of a prefragment is mainly decided by the nucleon-nucleon cross sections and the proton and neutron density distributions. Differently to the strictly linear increase of IYR(m) with x in SGC/CSE, IYR(m) of fragments with small x has very little difference but show accelerating changes in fragments with large x in SAA. This phenomena can be explained as the isospin effect in HIC, i.e., the similarity in IYR(m) of small x due to the similarity of proton and neutron density distributions in central collisions, while the large difference in IYR(m) of large x are corresponding to the large difference between the proton and neutron density distributions [7, 31, 33, 34]. The obvious IYR(m) dependence on the isospin of the projectile also exhibits the behavior of the "finite size" effects shown in SGC/CSE. But contrary to the the "finite size" effects in SGC/CSE, the dependence of IYR(m) on the system volume of projectile with same n/p is found to be very small.

Using one reaction, the extracted $(\mu_n - \mu_p)/T$ and a_c/T using the IYR method may depend on the n/p ratio of the projectile. In Huang's work[20], the a_c/T is scaled to the reaction system parameter Z/A($\equiv (Z_p + Z_t)/(A_p + A_t)$). If using the methods in Ref. [20] to extract the a_{sym}/T of fragments, an increase of 0.15 of a_c/T may introduce a difference of 0.6∼1.5 when x increase from 4 to 10, i.e., for fragment with small x, the difference is rather small. Based on these results, it is proposed the isobaric yield ratio has very little "finite-size" effects depending on the size of reaction system, and can be used to extract the coefficients of energy terms contributing to the free energy.

To summarize, the "finite size" effects in IYR(m) in SGC/CSE are revisited using a modified SAA model. The SAA results well reproduce the IYR(m) in the measured 140A MeV ^{40}Ca+^{9}Be reactions, while the SAA calculated IYR(m) is smaller than the experimental results in the 140A MeV ^{48}Ca+^{9}Be reaction. IYR(m) is found to depend on the isospin of projectile nuclei. IYR(m) saturates and its dependence on the isospin of projectile is weakened and even disappears in reaction of very neutron-rich nucleus. The "finite-size" effect shown in GC/SCE disappears in the SAA results. The IYR(m) depends on the isospin of the projectile rather than the size of reaction system shown in the results of SGC/CSE.

ACKNOWLEDGMENTS

This work is partially supported by National Natural Science Foundation of China under contract Nos. 10905017 and 11035009, Program for Innovative Research Team (in Science and Technology) under Grant No. 2010IRTSTHN002 in Universities of Henan Province, China, Shanghai Development Foundation for Science and Technology under contract No. 09JC1416800, and the Knowledge Innovation Project of the Chinese Academy of Sciences under grant No. KJCX2-EW-N01, and the Young Teacher Project in Henan Normal University, China.

[1] J. B. Natowitz *et al.*, Phys. Rev. C **52**, R2322 (1995).

[2] J. Wang *et al.*, Phys. Rev. C **72**, 024603 (2005).

[3] Y. G. Ma *et al.*, Phys. Rev. C **71**, 054606 (2005).

[4] R. Wada *et al.*, Phys. Rev. C **55**, 227 (1997).

[5] M. B. Tsang *et al.*, Phys. Rev. Lett. **85**, 716 (2000).

[6] P. Zhou *et al.*, Phys. Rev. C **84**, 037605 (2011).

[7] D. Q. Fang *et al.*, J. Phys. G: Nucl. Part. Phys., **34** (2007) 2173.

[8] Z. Chen *et al.*, Phys. Rev. C **81**, 064613 (2010).

[9] Y. G. Ma *et al.*, Phys. Rev. C **72**, 064603 (2005).

[10] S. R. Souza *et al.*, Phys. Rev. C **78**, 014605 (2008).

[11] S. R. Souza *et al.*, Phys. Rev. C **80**, 044606 (2009).

[12] C. O. Dorso *et al.*, Phys. Rev. C **73**, 044601 (2006).

[13] C. O. Dorso, Phys. Rev. C **73**, 034605 (2006).

[14] A. Ono *et al.*, Phys. Rev. C **68**, 051601(R) (2003).

[15] M. B. Tsang *et al.*, Eur. Phys. J. A **30**, 129 (2006).

[16] M. B. Tsang *et al.*, Phys. Rev. C **64**, 054615 (2001).

[17] A. S. Botvina, O. V. Lozhkin, and W. Trautmann, Phys. Rev. C **65**, 044610 (2002).

[18] R. W. Minich *et al.*, Phys. Lett. B **118**, (1982) 458.

[19] A. S. Hirsch *et al.*, Phys. Rev. C **29**, (1984) 508.

[20] M. Huang *et al.*, Phys. Rev. C **81**, 044620 (2010).

[21] C. W. Ma, F. Wang, Y. G. Ma and C. Jin, Phys. Rev. C **83**, 064620 (2011).

[22] S. R. Souza and M. B. Tsang, Phys. Rev. C 85, 024603 (2012).

[23] C. B. Das *et al.*, Phys. Rep. 406, 1 (2005).

[24] T. Brohm, and K. -H. Schmidt, Nucl. Phys. A **569**, 821 (1994).

[25] C. W. Ma *et al.*, Phys. Rev. C **79**, 034606 (2009).

[26] H. L. Wei, and C. W. Ma, Acta Phys. Sin. **59**, 5364 (2010) (in Chinese).

[27] J. J. Gaimard, and K. -H. Schmidt, Nucl. Phys. A **531**, 709 (1991).

[28] D. Q. Fang *et al.*, Phys. Rev. C, **81**, 047603 (2010).

[29] C.-W. Ma, H.-L. Wei, and M. Yu, Phys. Rev. C, **82**, 057602 (2010).

[30] D. Q. Fang *et al.*, Phys. Rev. C **61**, 044610 (2000).

[31] C. W. Ma, H. L. Wei, and J. Y. Wang, Chin. Phys. B **18**, 4781 (2009).

[32] C. W. Ma *et al.*, Chin. Phys. B, **17**, (2008) 1216.

[33] C. W. Ma J. Phys. G: Nucl. Part. Phys. **37**, 015104 (2010).

[34] C. W. Ma, and S. S. Wang, Chin. Phys. C **35**, 1017 (2011).

[35] M. Mocko *et al.*, Phys. Rev. C **74**, 054612 (2006).